

## PAPER

# Frequency-Interleaved Spread Spectrum with MMSE Frequency-Domain Equalization

Kazuaki TAKEDA<sup>†a)</sup>, Student Member and Fumiyuki ADACHI<sup>†b)</sup>, Member

**SUMMARY** The use of frequency-domain equalization (FDE) based on minimum mean square error (MMSE) criterion can significantly improve the downlink bit error rate (BER) performances of DS- and MC-CDMA in a frequency-selective fading channel. However, the uplink BER performance degrades due to a strong multi-user interference (MUI). In this paper, we propose frequency-interleaved spread spectrum (SS) using MMSE-FDE, in which the subcarrier components of each user's signal are interleaved onto a wider bandwidth. Then, the frequency-interleaved frequency-domain signal is transformed into a time-domain signal by the inverse fast Fourier transform (IFFT). Frequency-interleaving patterns assigned to different users are orthogonal to each other. The proposed scheme can avoid the MUI completely while achieving frequency diversity gain due to MMSE-FDE. It is shown by computer simulation that the use of frequency-interleaving can significantly improve the uplink performance in a frequency-selective Rayleigh fading channel.

**key words:** component, MMSE-FDE, frequency-interleaving

## 1. Introduction

There have been tremendous demands for high-speed data transmissions in mobile communications [1]. A mobile communication channel is composed of many distinct propagation paths having different time delays, resulting in a frequency-selective fading channel [2]. The hostile fading channel is a major obstacle to achieve high-speed and high-quality data transmissions. In a frequency-selective fading channel, inter-symbol interference (ISI) is produced and the bit error rate (BER) performance significantly degrades when single carrier (SC) transmission is used without using equalization technique. Direct sequence code division multiple access (DS-CDMA), which is classified as the SC transmission technique, is adopted in the present cellular mobile communication systems for data transmissions of up to around a few Mbps [3]. DS-CDMA can exploit the channel frequency-selectivity by the use of coherent rake combining that resolves the propagation paths having different time delays and then coherently combines them to get the path diversity gain [4]. Recently, a lot of research attention is paid to the next generation mobile communication systems that will support transmission data rates higher than few tens of Mbps [5]. However, the wireless channel for such high speed data transmission becomes

severely frequency-selective and the BER performance with rake combining degrades due to a strong inter-path interference. Hence, the use of some advanced channel equalization technique is indispensable.

Multi-carrier (MC)-CDMA can exploit the channel frequency-selectivity by using simple one-tap frequency-domain equalization (FDE) based on minimum mean square error (MMSE) criterion and therefore, has been attracting much attention for the downlink transmission [6]–[8]. Recently, DS-CDMA has been considered again, but with the application of FDE as in MC-CDMA. It was shown [9]–[11] that MMSE-FDE can replace rake combining to significantly improve the downlink BER performance of DS-CDMA and give a similar BER performance to MC-CDMA. However, for both DS- and MC-CDMA uplink transmissions, different user's signal goes through different propagation channels and hence, a BER floor is produced due to a strong multi-user interference (MUI) even if MMSE-FDE is applied [12]. To avoid MUI, some technique (e.g., MUI cancellation and pre-equalization) is necessary [13]. Quite recently, chip repetition DS-CDMA has been proposed that uses comb-like spectrum to avoid the spectrum overlapping among different users [14], [15].

If different users' spectra are interleaved and spread over a wider bandwidth so as not to overlap, the MUI can be eliminated. In this paper, frequency-interleaved spread spectrum (SS) using MMSE-FDE is proposed to avoid the MUI completely and improve the uplink performance. In the proposed scheme, the subcarrier components of each user's SS signal are interleaved, using orthogonal interleaving patterns, onto a wider bandwidth. Then, the frequency-interleaved SS signal is transformed into a time-domain signal by inverse fast Fourier transform (IFFT). Orthogonal frequency-interleaving patterns are assigned to different users. The proposed scheme can avoid MUI completely while maximizing the frequency diversity gain owing to MMSE-FDE. The uplink BER performance of the proposed scheme is evaluated by computer simulation in a frequency-selective Rayleigh fading channel. When frequency-interleaving is used, the transmit signal power varies in the time-domain even in SC transmission, thereby producing the peak-to-average power ratio (PAPR) problem similar to MC transmission. The PAPR of the frequency-interleaved SS signals is also discussed.

The remainder of this paper is organized as follows. Section 2 presents the uplink transmission system model of the frequency-interleaved SS with MMSE-FDE. The de-

Manuscript received October 11, 2005.

Manuscript revised May 30, 2006.

<sup>†</sup>The authors are with the Department of Electrical and Communication Engineering, Graduate School of Engineering, Tohoku University, Sendai-shi, 980-8579 Japan.

a) E-mail: [takeda@mobile.ecei.tohoku.ac.jp](mailto:takeda@mobile.ecei.tohoku.ac.jp)

b) E-mail: [adachi@ecei.tohoku.ac.jp](mailto:adachi@ecei.tohoku.ac.jp)

DOI: 10.1093/ietcom/e90-b.2.260

sign of frequency-interleaving pattern is discussed in Sect. 3. In Sect. 4, the simulated BER performance of the proposed frequency-interleaved SS is evaluated by computer simulation. Section 5 gives some conclusions.

## 2. Frequency-Interleaved SS with MMSE-FDE

### 2.1 Overall Transmission System

Figure 1 shows the uplink transmitter/receiver for single-carrier (SC)-SS using frequency-interleaving. We assume that  $U$  users are transmitting their data to the base station. At the  $u$ th user's ( $u = 0 \sim U - 1$ ) mobile transmitter, after turbo encoding, a binary data sequence is transformed into a data modulated symbol sequence and is divided into a sequence of blocks of  $N_c/SF_t$  symbols each, where  $N_c$  is the FFT window size and  $SF_t$  is the spreading factor. Then, the symbol sequence  $\{d^{(u)}(n); n = 0 \sim N_c/SF_t - 1\}$  in each block is spread by a spreading sequence  $\{c^{(u)}(t); t = \dots, -1, 0, 1, \dots\}$  of spreading factor  $SF_t$ . The resulting  $N_c$ -chip sequence in each block is decomposed by  $N_c$ -point FFT into frequency-domain signal  $\mathbf{S}^{(u)} = \{S^{(u)}(k); k = 0 \sim N_c - 1\}$ .  $\mathbf{S}^{(u)}$  is interleaved onto an  $SF_f$  times wider bandwidth of  $N_c SF_f$  subcarriers [16]. Here, the overall spreading factor  $SF$  is given by  $SF = SF_t SF_f$ . Interleaving patterns are determined so that different users' subcarrier components do not overlap with each other (see Fig. 2). Finally,  $N_c SF_f$ -point IFFT is applied to obtain the frequency-interleaved time-domain chip sequence of  $N_c SF_f$  chips. The last  $N_g$  chips of each chip block are copied and inserted, as a cyclic prefix, into the guard interval (GI) at the beginning of each block to form a block of  $N_c SF_f + N_g$  chips.

The frequency-interleaved SC-SS chip block is transmitted over a frequency-selective fading channel and is received at a base station receiver. The received chip sequence is decomposed by  $N_c SF_f$ -point FFT into  $N_c SF_f$  subcarrier components. Then, MMSE-FDE is carried out and frequency de-interleaving is performed to extract each user's frequency-domain signal. Finally,  $N_c$ -point IFFT is applied to obtain the time-domain chip block for despreading and turbo decoding.

When  $U$  users communicate with a base station, the choice of  $(SF_t, SF_f)$  is important for a given  $SF$ .  $(SF_t, SF_f)$  is chosen as follows; first  $SF_f$  is set as  $SF_f = U$  so that different users' frequency components do not overlap with each other. Then,  $SF_t$  is set as  $SF_t = SF/U$  to suppress the residual inter-chip interference (ICI) produced after MMSE-FDE. The reason why we set  $SF_f$  first is that the MUI is the predominant cause of the performance degradation rather than the residual ICI. The above choice of  $(SF_t, SF_f)$  shows the best trade off between suppressing the residual ICI and suppressing the MUI. This is confirmed by computer simulation in Sect. 4.

The same transmitting/receiving processing can be applied to multi-carrier (MC)-SS by just removing  $N_c$ -point FFT and IFFT from the transmitter and the receiver, respectively [17].

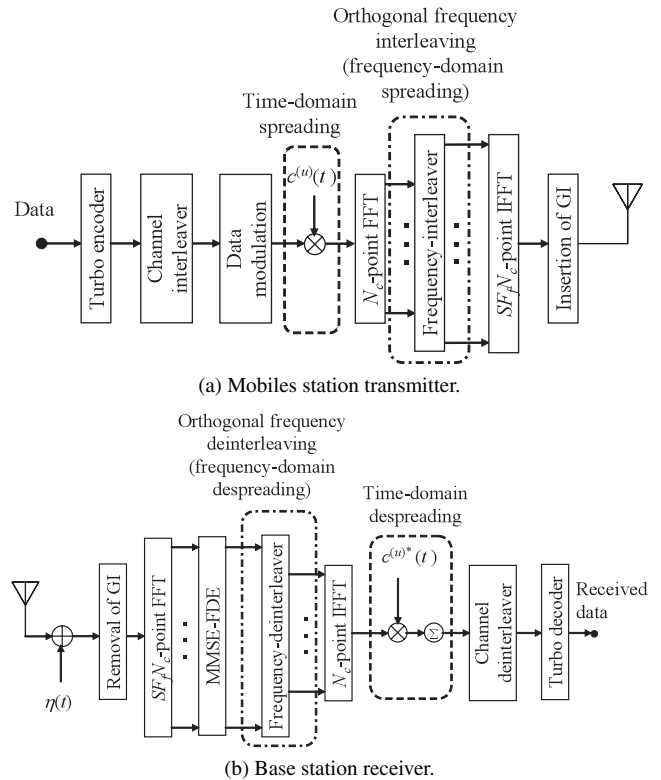


Fig. 1 Uplink transmitter/receiver for frequency-interleaved SC-SS.

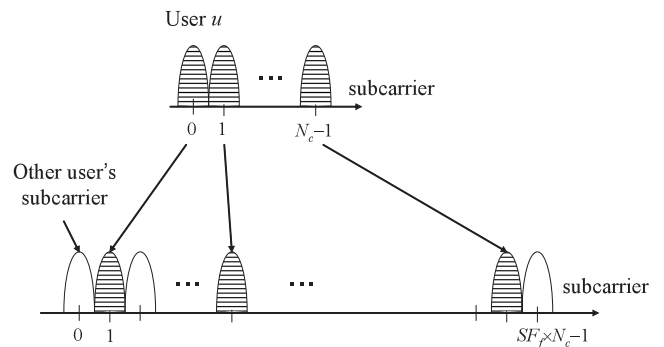


Fig. 2 Frequency-interleaving.

### 2.2 Transmit Signal Representaion

First, we consider SC-SS. Throughout this paper, the chip-spaced time representation of transmit signals is used. Without loss of generality, transmission of data symbol sequence  $\{d^{(u)}(n); n = 0 \sim N_c/SF_t - 1\}$  in one block is considered, where  $|d^{(u)}(n)| = 1$ . The chip sequence after spreading is expressed, using vector representation, as  $\mathbf{s}_{SC}^{(u)} = [s_{SC}^{(u)}(0), \dots, s_{SC}^{(u)}(t), \dots, s_{SC}^{(u)}(N_c - 1)]^T$ , where T denotes the transposition.  $s_{SC}^{(u)}(t)$  can be expressed, using the equivalent lowpass representation, as

$$s_{SC}^{(u)}(t) = \sqrt{2E_s/(T_c SF_t)} d^{(u)}(\lfloor t/SF_t \rfloor) c(t), \quad (1)$$

where  $E_s$  and  $T_c$  denote the symbol energy and the chip du-

ration, respectively.

$s_{\text{SC}}^{(u)}$  is decomposed by  $N_c$ -point FFT into frequency-domain signal  $S_{\text{SC}}^{(u)} = [S_{\text{SC}}^{(u)}(0), \dots, S_{\text{SC}}^{(u)}(k), \dots, S_{\text{SC}}^{(u)}(N_c-1)]^T$ , where  $S_{\text{SC}}^{(u)}(k)$  is the  $k$ th subcarrier component, given by

$$S_{\text{SC}}^{(u)}(k) = \sum_{t=0}^{N_c-1} s_{\text{SC}}^{(u)}(t) \exp\left(-j2\pi k \frac{t}{N_c}\right). \quad (2)$$

$S_{\text{SC}}^{(u)}$  is interleaved onto  $SF_f$  times wider bandwidth of  $N_c SF_f$  subcarriers. The resulting frequency-interleaved signal can be represented as

$$\begin{aligned} \hat{S}_{\text{SC}}^{(u)} &= [\hat{S}_{\text{SC}}^{(u)}(0), \dots, \hat{S}_{\text{SC}}^{(u)}(k'), \dots, \hat{S}_{\text{SC}}^{(u)}(N_c SF_f - 1)]^T \\ &= \mathbf{Q}^{(u)} S_{\text{SC}}^{(u)}, \end{aligned} \quad (3)$$

where  $\mathbf{Q}^{(u)}$  is an  $(N_c SF_f)$ -by- $N_c$  frequency-interleaving matrix.

Interleaving patterns are determined so that different users' subcarrier components do not overlap with each other (see Fig. 2).  $\mathbf{Q}^{(u)}$  must satisfy

$$\{\mathbf{Q}^{(u)}\}^T \mathbf{Q}^{(u')} = \begin{cases} \mathbf{I} & \text{if } u = u' \\ \mathbf{0} & \text{otherwise} \end{cases}, \quad (4)$$

where  $\mathbf{I}$  is an  $N_c \times N_c$  identity matrix. Below, an example is shown for the case of  $SF_f = 2$  and  $N_c = 4$  for multiplexing two users ( $u = 0$  and 1). The following interleaving matrices,  $\mathbf{Q}^{(0)}$  and  $\mathbf{Q}^{(1)}$ , can be used:

$$\mathbf{Q}^{(0)} = \begin{pmatrix} 0 & 0 & 0 & 0 \\ 0 & 1 & 0 & 0 \\ 0 & 0 & 0 & 1 \\ 0 & 0 & 0 & 0 \\ 0 & 0 & 1 & 0 \\ 0 & 0 & 0 & 0 \\ 0 & 0 & 0 & 0 \\ 0 & 0 & 0 & 0 \\ 1 & 0 & 0 & 0 \end{pmatrix}, \quad \mathbf{Q}^{(1)} = \begin{pmatrix} 0 & 0 & 1 & 0 \\ 0 & 0 & 0 & 0 \\ 0 & 0 & 0 & 0 \\ 0 & 1 & 0 & 0 \\ 0 & 0 & 0 & 0 \\ 0 & 0 & 1 & 0 \\ 1 & 0 & 0 & 0 \\ 0 & 0 & 0 & 0 \end{pmatrix}. \quad (5)$$

Positions of "1" for  $\mathbf{Q}^{(0)}$  and  $\mathbf{Q}^{(1)}$  are not overlapping and therefore  $\mathbf{Q}^{(0)}$  and  $\mathbf{Q}^{(1)}$  are orthogonal to each other.

Finally,  $N_c SF_f$ -point IFFT is applied to obtain the frequency-interleaved SC-SS signal  $\hat{s}_{\text{SC}}^{(u)}(t')$ ,  $t' = 0 \sim (N_c SF_f - 1)$ , which can be expressed as

$$\hat{s}_{\text{SC}}^{(u)}(t') = \frac{1}{N_c} \sum_{k'=0}^{N_c SF_f - 1} \hat{S}_{\text{SC}}^{(u)}(k') \exp\left(j2\pi k' \frac{t'}{N_c SF_f}\right). \quad (6)$$

Next we consider MC-SS. The  $k$ th subcarrier component is given by

$$s_{\text{MC}}^{(u)}(k) = \sqrt{2E_s / (T_c SF_f N_c)} d^{(u)}(\lfloor k / SF_f \rfloor) c(k). \quad (7)$$

$s_{\text{MC}}^{(u)} = [s_{\text{MC}}^{(u)}(0), \dots, s_{\text{MC}}^{(u)}(k), \dots, s_{\text{MC}}^{(u)}(N_c - 1)]^T$  is interleaved onto  $SF_f$  times wider bandwidth as in SC-SS. The resulting frequency-interleaved signal is represented as

$$\hat{s}_{\text{MC}}^{(u)} = \mathbf{Q}^{(u)} s_{\text{MC}}^{(u)}. \quad (8)$$

$N_c SF_f$ -point IFFT is applied to obtain the frequency-interleaved MC-SS signal  $\hat{s}_{\text{MC}}^{(u)}(t')$ ,  $t' = 0 \sim (N_c SF_f - 1)$ , which can be expressed as

$$\hat{s}_{\text{MC}}^{(u)}(t') = \sum_{k'=0}^{N_c SF_f - 1} \hat{s}_{\text{MC}}^{(u)}(k') \exp\left(j2\pi k' \frac{t'}{N_c SF_f}\right). \quad (9)$$

After the GI insertion, the frequency-interleaved SC- or MC-SS signal is transmitted over a frequency-selective fading channel.

### 2.3 Received Signal Representation

We assume a block fading so that the path gains remain constant over one block length of  $(N_c SF_f + N_g)$  chips. Assuming that the channel has  $L$  independent propagation paths with  $T_c$ -spaced distinct time delays  $\{\tau_l; l = 0 \sim L - 1\}$ , the discrete-time impulse response  $h^{(u)}(t')$  of the  $u$ th user multipath channel is expressed as [18]

$$h^{(u)}(t') = \sum_{l=0}^{L-1} h_l^{(u)} \delta(t' - \tau_l), \quad (10)$$

where  $h_l^{(u)}$  is the  $l$ th path gain with  $\sum_{l=0}^{L-1} E[|h_l^{(u)}|^2] = 1$  ( $E[\cdot]$  denotes the ensemble average operation). It is assumed that the maximum time delay difference of the channel is shorter than the GI.

The received signal  $r_{\text{SC(or MC)}}(t')$ ,  $t' = -N_g \sim (N_c SF_f - 1)$ , at the base station is expressed as

$$r_{\text{SC(or MC)}}(t') = \sum_{u=0}^{U-1} \sum_{l=0}^{L-1} h_l^{(u)} \hat{s}_{\text{SC(or MC)}}^{(u)}(t' - \tau_l) + \eta(t'), \quad (11)$$

where  $\eta(t')$  is a zero-mean complex Gaussian noise process having a variance of  $2N_0 SF_f / T_c$  with  $N_0$  being the single-sided power spectrum density of the additive white Gaussian noise (AWGN).

### 2.4 MMSE-FDE and Frequency-Deinterleaving

The received signal  $r(t')$  is decomposed by  $N_c SF_f$ -point FFT into  $N_c SF_f$  subcarrier components  $\{R_{\text{SC(or MC)}}(k'); k' = 0 \sim (N_c SF_f - 1)\}$ . The  $k'$ th subcarrier component  $R_{\text{SC(or MC)}}(k')$  is given by

$$\begin{cases} R_{\text{SC}}(k') = \sum_{t'=0}^{N_c SF_f - 1} r_{\text{SC}}(t') \exp\left(-j2\pi k' \frac{t'}{N_c SF_f}\right) \\ \quad = \sum_{u=0}^{U-1} SF_f H^{(u)}(k') \hat{s}_{\text{SC}}^{(u)}(k') + \Pi(k') \\ R_{\text{MC}}(k') = \sum_{t'=0}^{N_c SF_f - 1} r_{\text{MC}}(t') \exp\left(-j2\pi k' \frac{t'}{N_c SF_f}\right) \\ \quad = N_c SF_f \sum_{u=0}^{U-1} H^{(u)}(k') \hat{s}_{\text{MC}}^{(u)}(k') + \Pi(k'), \end{cases} \quad (12)$$

where  $H^{(u)}(k')$  and  $\Pi(k')$  are the channel gain and the noise component due to the AWGN, respectively, and they are given by

$$\begin{cases} H^{(u)}(k') = \sum_{l=0}^{L-1} h_l^{(u)} \exp\left(-j2\pi k' \frac{\tau_l}{N_c S F_f}\right) \\ \Pi(k') = \sum_{t'=0}^{N_c S F_f - 1} \eta(t') \exp\left(-j2\pi k' \frac{t'}{N_c S F_f}\right). \end{cases} \quad (13)$$

Without loss of generality, detection of the 0th ( $u = 0$ ) user's data sequence is considered. MMSE-FDE is carried out to obtain

$$\hat{R}_{\text{SC(or MC)}}^{(0)}(k') = R_{\text{SC(or MC)}}(k') w^{(0)}(k'), \quad (14)$$

where  $w^{(0)}(k')$  is the MMSE equalization weight at the  $k'$ th subcarrier. It is given by [8]

$$w^{(0)}(k') = \frac{H^{(0)*}(k')}{|H^{(0)}(k')|^2 + \left(\frac{1}{S F_f} \frac{E_s}{N_0}\right)^{-1}}, \quad (15)$$

where  $E_s/N_0$  is the average symbol energy-to-AWGN power spectrum density ratio and  $*$  denotes the complex conjugate operation. Substituting Eq. (12) into Eq. (14), we have

$$\begin{cases} \hat{R}_{\text{SC}}^{(0)}(k') = S F_f \sum_{u=0}^{U-1} w^{(u)}(k') H^{(u)}(k') \hat{S}_{\text{SC}}^{(u)}(k') \\ \quad + w^{(0)}(k') \Pi(k') \\ \quad = S F_f \sum_{u=0}^{U-1} \tilde{H}^{(u)}(k') \hat{S}_{\text{SC}}^{(u)}(k') + \tilde{\Pi}(k') \\ \hat{R}_{\text{MC}}^{(0)}(k') = N_c S F_f \sum_{u=0}^{U-1} w^{(u)}(k') H^{(u)}(k') \hat{S}_{\text{MC}}^{(u)}(k') \\ \quad + w^{(0)}(k') \Pi(k') \\ \quad = N_c S F_f \sum_{u=0}^{U-1} \tilde{H}^{(u)}(k') \hat{S}_{\text{MC}}^{(u)}(k') + \tilde{\Pi}(k'), \end{cases} \quad (16)$$

where  $\tilde{H}^{(u)}(k')$  and  $\tilde{\Pi}(k')$  are the equivalent channel gain and the noise component after MMSE-FDE, respectively.  $\tilde{H}^{(u)}(k')$  and  $\tilde{\Pi}(k')$  are given by

$$\begin{cases} \tilde{H}^{(u)}(k') = w^{(0)}(k') H^{(u)}(k') \\ \tilde{\Pi}(k') = w^{(0)}(k') \Pi(k'). \end{cases} \quad (17)$$

Using the vector representation  $\hat{R}_{\text{SC(or MC)}}^{(0)} = [\hat{R}_{\text{SC(or MC)}}^{(0)}(0), \dots, \hat{R}_{\text{SC(or MC)}}^{(0)}(N_c S F_f - 1)]^T$ , Eq. (16) can be rewritten as

$$\begin{cases} \hat{R}_{\text{SC}}^{(0)} = S F_f \sum_{u=0}^{U-1} \tilde{H}^{(u)} \hat{S}_{\text{SC}}^{(u)} + \tilde{\Pi} \\ \hat{R}_{\text{MC}}^{(0)} = N_c S F_f \sum_{u=0}^{U-1} \tilde{H}^{(u)} \hat{S}_{\text{MC}}^{(u)} + \tilde{\Pi}, \end{cases} \quad (18)$$

where  $\tilde{H}^{(u)}$  and  $\tilde{\Pi}$  are  $(N_c S F_f)$ -by- $(N_c S F_f)$  equivalent channel gain matrix and  $(N_c S F_f)$ -by-1 noise vector after MMSE-FDE, respectively. They are represented as

$$\begin{cases} \tilde{H}^{(u)} = \text{diag}(\tilde{H}^{(u)}(0), \dots, \tilde{H}^{(u)}(k'), \dots, \tilde{H}^{(u)}(S F_f N_c - 1)) \\ \tilde{\Pi} = [\tilde{\Pi}(0), \dots, \tilde{\Pi}(k'), \dots, \tilde{\Pi}(S F_f N_c - 1)]^T. \end{cases} \quad (19)$$

$\hat{R}_{\text{SC(or MC)}}^{(0)}$  is deinterleaved to extract the 0th user's frequency-domain signal  $\tilde{R}_{\text{SC(or MC)}}^{(0)} = [\tilde{R}_{\text{SC(or MC)}}^{(0)}(0), \dots, \tilde{R}_{\text{SC(or MC)}}^{(0)}(N_c - 1)]^T$ . Using Eqs. (3) and (8) for SC-SS and MC-SS, respectively, and Eq. (18),  $\tilde{R}_{\text{SC(or MC)}}^{(0)}$  is given by

$$\begin{cases} \tilde{R}_{\text{SC}}^{(0)} = \mathbf{Q}^{(0)T} \hat{R}_{\text{SC}}^{(0)} \\ \quad = S F_f \sum_{u=0}^{U-1} \left\{ \mathbf{Q}^{(0)T} \tilde{H}^{(u)} \mathbf{Q}^{(u)} \right\} \mathbf{s}_{\text{SC}}^{(u)} + \mathbf{Q}^{(0)T} \tilde{\Pi} \\ \tilde{R}_{\text{MC}}^{(0)} = \mathbf{Q}^{(0)T} \hat{R}_{\text{MC}}^{(0)} \\ \quad = N_c S F_f \sum_{u=0}^{U-1} \left\{ \mathbf{Q}^{(0)T} \tilde{H}^{(u)} \mathbf{Q}^{(u)} \right\} \mathbf{s}_{\text{MC}}^{(u)} + \mathbf{Q}^{(0)T} \tilde{\Pi}. \end{cases} \quad (20)$$

Since the frequency-interleaving matrices  $\mathbf{Q}^{(u)}$ ,  $u = 0 \sim U - 1$ , are orthogonal (see Eq. (4)) and  $\tilde{H}^{(u)}$  is a diagonal matrix,  $\mathbf{Q}^{(u')T} \tilde{H}^{(u)} \mathbf{Q}^{(u)}$  satisfies

$$\mathbf{Q}^{(u')T} \tilde{H}^{(u)} \mathbf{Q}^{(u)} = \begin{cases} \mathbf{Q}^{(u')T} \tilde{H}^{(u')} \mathbf{Q}^{(u')} & \text{if } u = u' \\ \mathbf{0} & \text{otherwise.} \end{cases} \quad (21)$$

Hence, we obtain

$$\begin{cases} \tilde{R}_{\text{SC}}^{(0)} = S F_f \left\{ \mathbf{Q}^{(0)T} \tilde{H}^{(0)} \mathbf{Q}^{(0)} \right\} \mathbf{s}_{\text{SC}}^{(0)} + \mathbf{Q}^{(0)T} \tilde{\Pi} \\ \tilde{R}_{\text{MC}}^{(0)} = N_c S F_f \left\{ \mathbf{Q}^{(0)T} \tilde{H}^{(0)} \mathbf{Q}^{(0)} \right\} \mathbf{s}_{\text{MC}}^{(0)} + \mathbf{Q}^{(0)T} \tilde{\Pi}, \end{cases} \quad (22)$$

where  $\left\{ \mathbf{Q}^{(0)T} \tilde{H}^{(0)} \mathbf{Q}^{(0)} \right\}$  is an  $N_c$ -by- $N_c$  diagonal matrix of the deinterleaved equivalent channel gains. It is understood from Eq. (22) that  $\mathbf{s}_{\text{SC}}^{(0)}$  is perfectly extracted without MUI since  $\left\{ \mathbf{Q}^{(0)T} \tilde{H}^{(0)} \mathbf{Q}^{(0)} \right\}$  is a diagonal matrix.

In SC-SS,  $N_c$ -point IFFT is applied to  $\tilde{R}_{\text{SC}}^{(0)}$  to obtain the time-domain chip sequence  $\{\tilde{r}_{\text{SC}}^{(0)}(t); t = 0 \sim (N_c - 1)\}$ :

$$\tilde{r}_{\text{SC}}^{(0)}(t) = \frac{1}{N_c} \sum_{k=0}^{N_c-1} \tilde{R}_{\text{SC}}^{(0)}(k) \exp\left(j2\pi t \frac{k}{N_c}\right). \quad (23)$$

Finally, despreading is carried out on  $\tilde{r}_{\text{SC}}^{(0)}(t)$ . In MC-SS, on the other hand, despreading is carried out on the deinterleaved chip sequence  $\tilde{R}_{\text{MC}}^{(0)}$ . We have

$$\begin{cases} \tilde{d}_{\text{SC}}^{(0)}(n) = \frac{1}{S F_f} \sum_{t=n S F_f}^{(n+1) S F_f - 1} \tilde{r}_{\text{SC}}^{(0)}(t) c^{(0)*}(t) \\ \tilde{d}_{\text{MC}}^{(0)}(n) = \frac{1}{S F_f} \sum_{k=n S F_f}^{(n+1) S F_f - 1} \tilde{R}_{\text{MC}}^{(0)}(k) c^{(0)*}(k), \end{cases} \quad (24)$$

which are the decision variables for data-demodulation on  $d^{(0)}(n)$  for SC and MC transmissions.

### 3. Frequency-Interleaving

#### 3.1 Frequency-Interleaving Patterns

In this paper, we consider three frequency-interleaving patterns: a) equal-space, b) block and c) random, as shown in Fig. 3. In equal-space interleaving, each user's subcarriers are periodically interleaved onto the entire bandwidth (see Fig. 3(a)) and therefore, a large frequency diversity gain can be obtained. The  $(p, q)$ -th element of  $\mathbf{Q}^{(u)}$  of Eq. (4) is given by

$$[\mathbf{Q}^{(u)}]_{p,q} = \begin{cases} 1 & \text{if } q=0 \sim (N_c - 1) \text{ and } p=SF_f \times q + u \\ 0 & \text{otherwise} \end{cases} \quad (25)$$

for equal-space interleaving and

$$[\mathbf{Q}^{(u)}]_{p,q} = \begin{cases} 1, & \text{if } q = 0 \sim (N_c - 1), p = N_c \times u + q \\ 0, & \text{otherwise} \end{cases} \quad (26)$$

for block interleaving. For example, when  $SF_f = 2$  and  $N_c = 4$ , two users can be orthogonally multiplexed. The interleaving matrices,  $\mathbf{Q}^{(0)}$  and  $\mathbf{Q}^{(1)}$ , can be

$$\mathbf{Q}^{(0)} = \begin{pmatrix} 1 & 0 & 0 & 0 \\ 0 & 0 & 0 & 0 \\ 0 & 1 & 0 & 0 \\ 0 & 0 & 0 & 0 \\ 0 & 0 & 1 & 0 \\ 0 & 0 & 0 & 0 \\ 0 & 0 & 0 & 0 \\ 0 & 0 & 0 & 1 \\ 0 & 0 & 0 & 0 \end{pmatrix}, \quad \mathbf{Q}^{(1)} = \begin{pmatrix} 0 & 0 & 0 & 0 \\ 1 & 0 & 0 & 0 \\ 0 & 0 & 0 & 0 \\ 0 & 1 & 0 & 0 \\ 0 & 0 & 0 & 0 \\ 0 & 0 & 1 & 0 \\ 0 & 0 & 0 & 0 \\ 0 & 0 & 0 & 0 \\ 0 & 0 & 0 & 1 \end{pmatrix} \quad (27)$$

for equal-space interleaving and

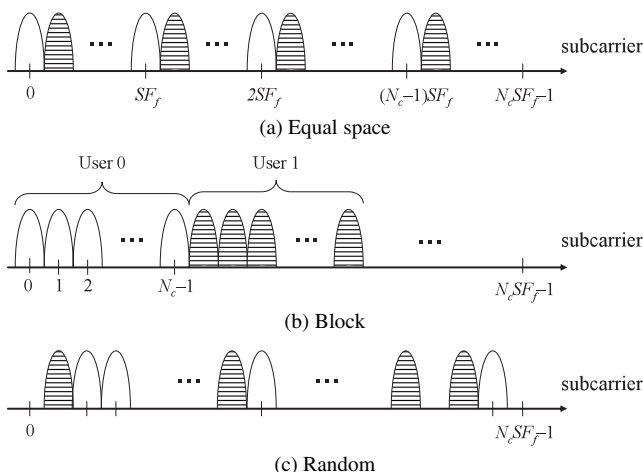


Fig. 3 Interleaving pattern.

$$\mathbf{Q}^{(0)} = \begin{pmatrix} 1 & 0 & 0 & 0 \\ 0 & 1 & 0 & 0 \\ 0 & 0 & 1 & 0 \\ 0 & 0 & 0 & 1 \\ 0 & 0 & 0 & 0 \\ 0 & 0 & 0 & 0 \\ 0 & 0 & 0 & 0 \\ 0 & 0 & 0 & 0 \\ 0 & 0 & 0 & 0 \end{pmatrix}, \quad \mathbf{Q}^{(1)} = \begin{pmatrix} 0 & 0 & 0 & 0 \\ 0 & 0 & 0 & 0 \\ 0 & 0 & 0 & 0 \\ 0 & 0 & 0 & 0 \\ 1 & 0 & 0 & 0 \\ 0 & 1 & 0 & 0 \\ 0 & 0 & 1 & 0 \\ 0 & 0 & 0 & 1 \\ 0 & 0 & 0 & 1 \end{pmatrix} \quad (28)$$

for block interleaving. In random interleaving,  $N_c$  rows of  $N_c$ -by- $N_c$  identity matrix are randomly permuted over  $SF_f N_c$  rows of  $(SF_f N_c)$ -by- $N_c$  matrix, but so as not to overlap with other users. An example of random interleaving has been given by Eq. (5).

#### 3.2 Time-Domain Signal Representation of Equal-Space Interleaving for SC-SS

When equal-space interleaving is applied to SC-SS signal, the  $k$ 'th subcarrier component  $\hat{S}_{SC}^{(u)}(k')$  after frequency-interleaving is given, from Eqs. (3) and (25), by

$$\hat{S}_{SC}^{(u)}(k') = \begin{cases} S_{SC}^{(u)}(k) & k' = SF_f k + u \text{ and } k = 0 \sim N_c - 1 \\ 0 & \text{otherwise.} \end{cases} \quad (29)$$

Substituting Eq. (29) into Eq. (6), we obtain

$$\tilde{s}_{SC}^{(u)}(t') = \frac{1}{N_c} \sum_{k=0}^{N_c-1} S_{SC}^{(u)}(k) \exp\left(j2\pi(SF_f k + u) \frac{t'}{N_c SF_f}\right). \quad (30)$$

Substitution of Eq. (2) into Eq. (30) gives

$$\begin{aligned} \hat{s}_{SC}^{(u)}(t') &= \frac{1}{N_c} \sum_{t=0}^{N_c-1} s_{SC}^{(u)}(t) \sum_{k=0}^{N_c-1} \exp\left(-j2\pi(t-t') \frac{k}{N_c}\right) \\ &\quad \times \exp\left(j2\pi t' \frac{u}{N_c SF_f}\right) \\ &= s_{SC}^{(u)}(t' \bmod N_c) \exp\left(j2\pi t' \frac{u}{N_c SF_f}\right), \end{aligned} \quad (31)$$

where  $(1/N_c) \sum_{k=0}^{N_c-1} \exp(-j2\pi t \frac{k}{N_c}) = \delta(t \bmod N_c)$  is used. It can be understood from Eq. (31) that equal-space interleaving of SC-SS can be performed in the time-domain by  $SF_f$  times repetition of the chip sequence  $\{s_{SC}^{(u)}(t); t = 0 \sim N_c - 1\}$ . The resulting interleaving pattern is exactly the same as that obtained by the chip repetition scheme (this does not require the FFT, frequency-interleaving and IFFT operations at the transmitter) proposed in [15].

### 4. Computer Simulation

Simulation parameters are summarized in Table 1. We consider quaternary phase shift keying (QPSK) data modulation, the overall spreading factor  $SF = SF_f SF_f = 16$  and the

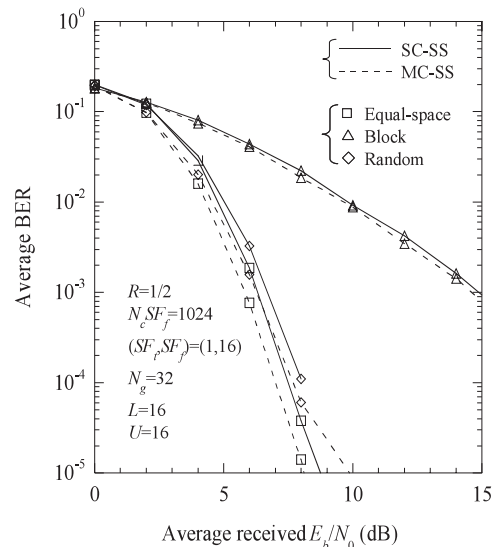
**Table 1** Simulation parameters.

Transmitter	Modulation	QPSK
	Spreading sequence	Long PN sequence
	Overall spreading factor	$SF = SF_t SF_f = 16$
	Allocation of spreading factor in time- and frequency-domains	$(SF_t, SF_f) = (1, 16), (4, 4), (16, 1)$
	Number of IFFT points	$N_c SF_f = 1024$
	GI	$N_g = 32$ (chips)
Turbo coding	$R = 1/2$ , (13,15)RSC encoder Log-MAP decoding with 8 iterations	
Channel	Fading	Frequency-selective block Rayleigh fading
	Power delay profile	$L = 16$ -path uniform power delay profile
Receiver	Frequency-domain equalization	MMSE
	Channel estimation	Ideal

number of subcarriers of the transmitted signal (or the number of IFFT points for the transmitter) is  $N_c SF_f = 1024$ . A long PN sequence of 4095 chips is used as a spreading code. The channel is assumed to be a frequency-selective block Rayleigh fading channel having  $L = 16$ -path uniform power delay profile (i.e.,  $E[|h_l|^2] = 1/L$  for all  $l$ ) with a time delay  $\tau_l$  of  $\tau_l = l$  chips. The path gain  $h_l$  is characterized by zero-mean complex Gaussian process and is generated using Jakes model [2] having 64 plane waves. A normalized maximum Doppler frequency of  $f_D T_c (N_c SF_f + N_g) = 0.004$  is assumed, where  $f_D = v/\lambda$  with  $v$  and  $\lambda$  representing respectively the mobile terminal traveling speed and the carrier frequency;  $f_D T_c (N_c SF_f + N_g) = 0.004$  corresponds to a terminal moving speed of 82 km/h for a chip rate of 100 Mcps, 5 GHz carrier frequency,  $N_c SF_f = 1024$  and  $N_g = 32$ . A  $R = 1/2$ -rate turbo code with a constraint length of 4 and decoding with 8 iterations are assumed. The information bit sequence length to be transmitted is taken to be 1024 bits. Perfect chip timing and ideal channel estimation are assumed. To obtain a similar frequency diversity gain to SC-SS, subcarriers of MC-SS are interleaved by an  $SF_t$ -by- $(N_c/SF_t)$  row-column block interleaver before frequency-interleaving.

#### 4.1 Comparison of Frequency-Interleaving Patterns

The uplink average BER performance achievable with joint frequency-interleaving and MMSE-FDE is plotted for SC- and MC-SS in Fig. 4 as a function of the average received energy-to-AWGN noise power spectrum density ratio  $E_b/N_0$ , given by  $E_b/N_0 = 0.5 (E_c/N_0) [1 + N_g/(N_c SF_f)]$ . We assume equal-space, block and random interleaving patterns. In random interleaving, a different random interleaving pattern is used every transmission of 1024 bits. As many as  $SF_f$  users can be multiplexed without MUI, hence,  $(SF_t, SF_f)$  is set as  $(SF_t, SF_f) = (1, 16)$  for  $U = 16$ . SC- and MC-SS with  $(SF_t, SF_f) = (1, 16)$  correspond to non-spread SC transmission and OFDMA, respectively. MC-SS

**Fig. 4** Average BER performances with equal-space, block and random frequency-interleaving.

provides a slightly better BER performance than SC-SS. In MC-SS, higher coding gain is achieved, while larger frequency diversity gain is obtained in SC-SS. However, in SC-SS, the residual inter-chip interference (ICI) is present after MMSE-FDE and this degrades the BER performance.

In both SC- and MC-SS, the equal-space interleaving is superior to the block and random interleavings. The block interleaving pattern provides the smallest frequency diversity gain (or smallest coding gain for MC-SS) since each user's subcarrier components remain consecutive. In random interleaving, some subcarrier components of the original signal may be mapped very closely, and hence the BER performance degrades since the frequency diversity gain reduces similar to the block interleaving. In equal-space interleaving, on the other hand, each user's subcarrier components are interleaved onto the entire bandwidth with equal spacing. Therefore, the largest frequency diversity gain can be obtained in SC-SS, while the largest coding gain can be achieved in MC-SS. According to our preliminary simulation, we found that the equal-space interleaving pattern gives the best performance. Hence, we consider only the equal-space interleaving pattern in the following simulations.

#### 4.2 Optimum Choice of $SF_f$ and $SF_t$

The uplink average BER performance achievable with joint frequency-interleaving and MMSE-FDE is plotted for SC- and MC-SS in Fig. 5. We consider three cases of  $(SF_t, SF_f)$ :  $(SF_t, SF_f) = (1, 16)$ ,  $(4, 4)$  and  $(16, 1)$ . The first case corresponds to the non-spread SC transmission and OFDMA. The third is equivalent to the pure DS- and MC-CDMA. It can be seen from Fig. 5 that SC-SS provides a slightly worse BER performance than MC-SS since the residual ICI is present after MMSE-FDE in SC-SS.

As many as  $U = SF_f$  users can access a base station

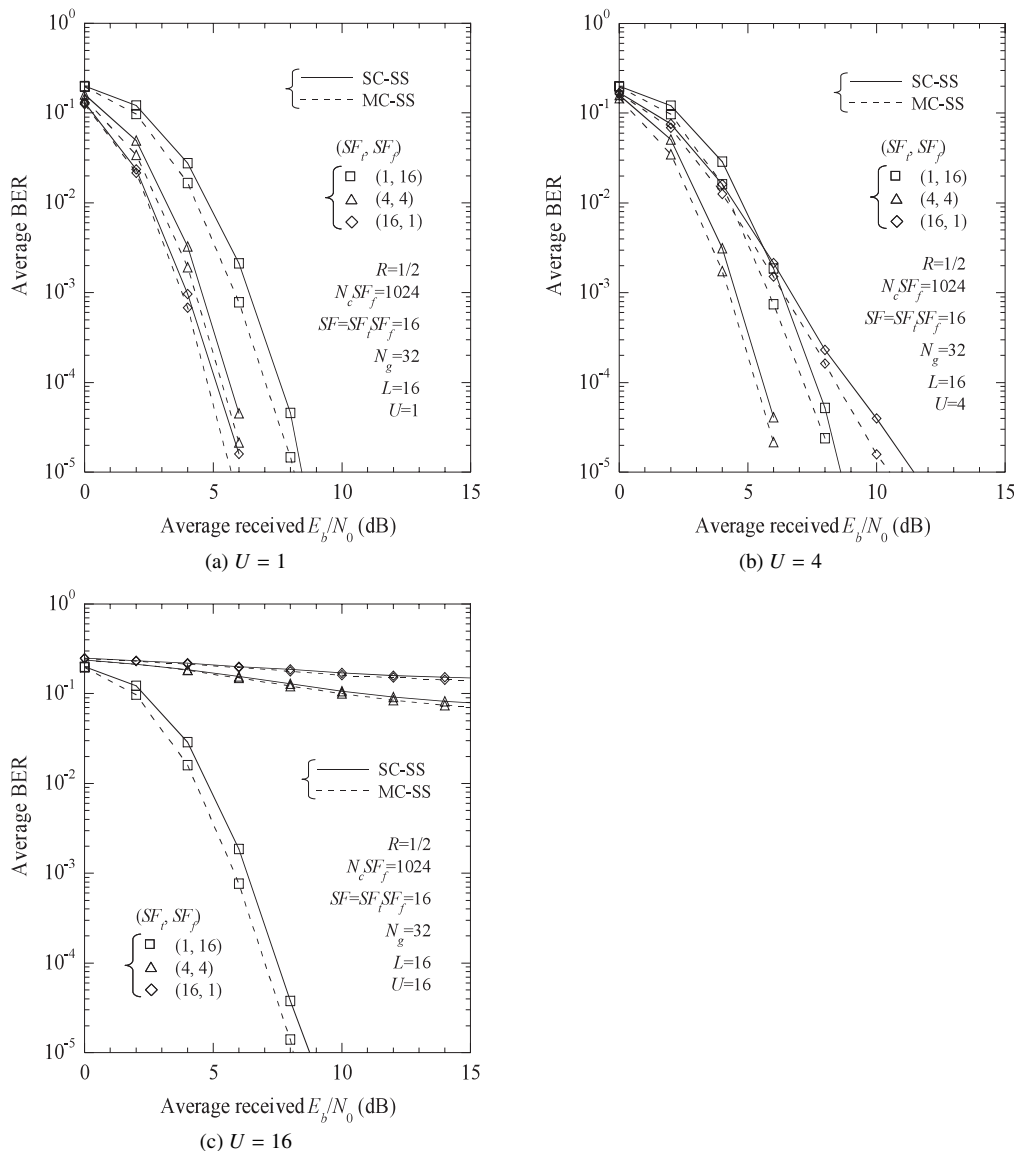


Fig. 5 Average BER performance with joint frequency-interleaving and MMSE-FDE.

without causing MUI at all. When  $U = 1$  (see Fig. 5(a)), the choice of  $(SF_t, SF_f) = (16, 1)$  provides the best BER performance. This is because, in SC-SS, the residual interchip interference (ICI) after MMSE-FDE can be best suppressed by time-domain despreading process, while in MC-SS, the largest frequency diversity gain can be obtained with  $(SF_t, SF_f) = (16, 1)$ . For the case of  $U = 4$  (see Fig. 5(b)), however, the BER performance degrades with  $(SF_t, SF_f) = (16, 1)$  because different users' subcarriers overlap and MUI is produced. With  $(SF_t, SF_f) = (4, 4)$ , the best BER performance is achieved due to MUI-free frequency-interleaving while reducing the residual ICI by time-domain despreading process. With  $(SF_t, SF_f) = (1, 16)$ , although the MUI can be avoided, the residual ICI cannot be all suppressed since the time-domain spreading is not used. When  $U = 16$  (see Fig. 5(c)), large BER floors are seen with  $(SF_t, SF_f) = (16, 1)$  and  $(4, 4)$  due to the MUI. On the other hand, with

$(SF_t, SF_f) = (1, 16)$ , no BER floor is seen and better BER performance than when  $(SF_t, SF_f) = (16, 1)$  and  $(4, 4)$  is achieved. This is because when  $(SF_t, SF_f) = (1, 16)$ , all users' subcarrier components do not overlap at all and the orthogonality among users is maintained. The  $E_b/N_0$  degradation in SC-SS (MC-SS) from the case of  $U = 1$  is 2.4 (2.3) dB for BER =  $10^{-4}$ . As a result, the optimum choice of  $(SF_t, SF_f)$  is  $(SF/U, U)$  for the given overall spreading factor  $SF$ .

#### 4.3 Discussion on PAPR

Figure 6 shows the complementary cumulative distribution function (CCDF) of the PAPR using frequency-interleaving with  $(SF_t, SF_f) = (1, 16)$  for SC- and MC-SS. PAPR is defined as the instantaneous peak transmit power in a block normalized by the average transmit power and is given, us-

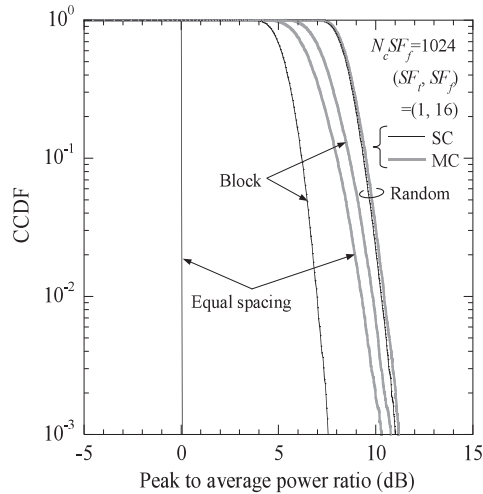


Fig. 6 CCDF of PAPR of frequency-interleaved SC- and MC-SS.

ing Eqs. (6) and (9) by

$$\text{PAPR} = \frac{\max_{0 \leq t' \leq N_c SF_f - 1} \left| \tilde{s}_{\text{SC(or MC)}}^{(u)}(t') \right|^2}{\frac{1}{N_c SF_f} E \left[ \sum_{t'=0}^{N_c SF_f - 1} \left| \tilde{s}_{\text{SC(or MC)}}^{(u)}(t') \right|^2 \right]}, \quad (32)$$

where  $E[\cdot]$  denotes the ensemble average operation, but it can be removed in our case since QPSK data modulation is used. SC-SS has a smaller PAPR than MC-SS irrespective of the frequency-interleaving patterns; the equal-space interleaving pattern of SC-SS gives the smallest PAPR among the three interleaving patterns. It can be understood from Eq. (31) that equal-space interleaving of SC-SS is equivalent to the chip repetition scheme [15].

## 5. Conclusion

In this paper, frequency-interleaved SS with MMSE-FDE has been proposed. The BER performance of the proposed system was evaluated by computer simulation. Higher coding gain is obtained in MC-SS, while a larger frequency diversity gain is obtained in SC-SS. However, in SC-SS, the residual ICI is present after MMSE-FDE and this degrades the BER performance. When  $U$  users access a base station, the choice of  $(SF_t, SF_f) = (SF/U, U)$  achieves the best BER performance due to MUI-free frequency-interleaving. When  $U = 16$ , both MC- and SC-SS provide almost identical BER performance; the  $E_b/N_0$  degradation in SC-SS (MC-SS) from the case of  $U = 1$  was found to be 2.4 (2.3) dB for  $\text{BER} = 10^{-4}$ . PAPR is also discussed when frequency-interleaving is applied. SC-SS always shows a smaller PAPR than MC-SS; no PAPR problem exists if the equal spacing frequency-interleaving is used in SC-SS.

## References

[1] F. Adachi, "Wireless past and future—Evolving mobile communications systems," IEICE Trans. Fundamentals, vol.E83-A, no.1,

pp.55–60, Jan. 2001.

[2] W.C., Jakes, Jr., ed., Microwave Mobile Communications, Wiley, New York, 1974.

[3] F. Adachi, M. Sawahashi, and H. Suda, "Wideband DS-CDMA for next generation mobile communications systems," IEEE Commun. Mag., vol.36, no.9, pp.56–69, Sept. 1998.

[4] J.G. Proakis, Digital Communications, 3rd ed., McGraw-Hill, 1995.

[5] Y. Kim et al., "Beyond 3G: Vision, requirements, and enabling technologies," IEEE Commun. Mag., vol.41, no.3, pp.120–124, March 2003.

[6] S. Hara and R. Prasad, "Overview of multicarrier CDMA," IEEE Commun. Mag., vol.35, no.12, pp.126–133, Dec. 1997.

[7] H. Atarashi, S. Abeta, and M. Sawahashi, "Variable spreading orthogonal frequency and code division multiplexing (VSF-OFCDM) for broadband packet wireless access," IEICE Trans. Commun., vol.E86-B, no.1, pp.291–299, Jan. 2003.

[8] M. Helard, R. Le Gouable, J.-F. Helard, and J.-Y. Baudais, "Multi-carrier CDMA techniques for future wideband wireless networks," Ann. Telecommun., vol.56, pp.260–274, 2001.

[9] K. Takeda, T. Itagaki, and F. Adachi, "Frequency-domain equalization for antenna diversity reception of DS-CDMA signals," Proc. 8th International Conference on Cellular and Intelligent Communications (CIC), Seoul, Korea, Oct. 2003.

[10] I. Martoyo, G.M.A. Sessler, J. Luber, and F.K. Jondral, "Comparing equalizers and multiuser detections for DS-CDMA downlink systems," Proc. IEEE VTC 2004 Spring, pp.1649–1653, May 2004.

[11] F. Adachi, D. Garg, S. Takaoka, and K. Takeda, "Broadband CDMA techniques," IEEE Wirel. Commun. Mag., vol.12, no.2, pp.8–18, April 2005.

[12] K. Takeda and F. Adachi, "MMSE frequency-domain equalization combined with space-time transmit diversity and antenna receive diversity for DS-CDMA," Proc. 59th IEEE Vehicular Technology Conference (VTC), pp.464–468, Milan, Italy, May 2004.

[13] S. Tomasin and N. Benvenuto, "Equalization and multiuser interference cancellation in CDMA systems," Proc. 6th International Symposium on WPMC, vol.1, pp.10–14, Yokosuka, Japan, Oct. 2003.

[14] M. Schnell, I. Broeck, and U. Sorger, "A promising new wideband multiple-access scheme for future mobile communications systems," Eur. Trans. Telecommun. (ETT), vol.10, no.4, pp.417–427, July/Aug. 1999.

[15] Y. Goto, T. Kawamura, H. Atarashi, and M. Sawahashi, "Variable spreading and chip repetition factors (VSCRF)-CDMA in reverse link for broadband wireless access," Proc. IEEE PIMRC2003, pp.254–259, Sept. 2003.

[16] K. Takeda and F. Adachi, "Multi-access method using frequency-interleaving and frequency-domain equalization for broadband mobile radio," IEICE Technical Report, RCS2004-143, Aug. 2004.

[17] K. Takeda and F. Adachi, "Multi-carrier multi-access using frequency-interleaving and its uplink BER performance," IEICE Technical Report, RCS2004-232, Nov. 2004.

[18] T.S. Rappaport, Wireless Communications, Prentice Hall, 1996.



**Kazuaki Takeda** received his B.E. and M.S. degrees in communications engineering from Tohoku University, Sendai, Japan, in 2003 and 2004, respectively. Currently he is a PhD student at the Department of Electrical and Communications Engineering, Graduate School of Engineering, Tohoku University. His research interests include equalization, interference cancellation, transmit/receive diversity, and multiple access techniques. He was a recipient of the 2003 IEICE RCS (Radio Communication Sys-

tems) Active Research Award and 2004 Inose Scientific Encouragement Prize.



**Fumiyuki Adachi** received the B.S. and Dr. Eng. degrees in electrical engineering from Tohoku University, Sendai, Japan, in 1973 and 1984, respectively. In April 1973, he joined the Electrical Communications Laboratories of Nippon Telegraph & Telephone Corporation (now NTT) and conducted various types of research related to digital cellular mobile communications. From July 1992 to December 1999, he was with NTT Mobile Communications Network, Inc. (now NTT DoCoMo, Inc.), where he

led a research group on wideband/broadband CDMA wireless access for IMT-2000 and beyond. Since January 2000, he has been with Tohoku University, Sendai, Japan, where he is a Professor of Electrical and Communication Engineering at the Graduate School of Engineering. His research interests are in CDMA wireless access techniques, equalization, transmit/receive antenna diversity, MIMO, adaptive transmission, and channel coding, with particular application to broadband wireless communications systems. From October 1984 to September 1985, he was a United Kingdom SERC Visiting Research Fellow in the Department of Electrical Engineering and Electronics at Liverpool University. Dr. Adachi served as a Guest Editor of IEEE JSAC on Broadband Wireless Techniques, October 1999, Wideband CDMA I, August 2000, Wideband CDMA II, Jan. 2001, and Next Generation CDMA Technologies, Jan. 2006. He is an IEEE Fellow and was a co-recipient of the IEEE Vehicular Technology Transactions Best Paper of the Year Award 1980 and again 1990 and also a recipient of Avant Garde award 2000. He was a recipient of IEICE Achievement Award 2002 and a co-recipient of the IEICE Transactions Best Paper of the Year Award 1996 and again 1998. He was a recipient of Thomson Scientific Research Front Award 2004.